Cavity QED photons for generating a double-cavity-induced transparency

Moteb M. Alqahtani
Department of Physics, King Khalid University, P.O. Box 960, Abha, Asir, 61421, Saudi Arabia

(Received 18 September 2023; accepted 8 February 2024; published 23 February 2024)

A method is presented for creating single- and double-cavity-induced transparency based on a cavity QED framework. Using this method we develop a fully quantized model of a cavity-induced transparency (CIT) scheme previously proposed [P. R. Rice and R. J. Brecha, Opt. Commun. **126**, 230 (1996)] adopting the quantum-jump approach. This allows us to analyze the interaction of N cavity fields with an $(N+1)$-level quantum system where $N = 2, 3$ for the cases of single- and double-cavity-induced transparency, respectively. In the steady-state limit, a general analytic expression for the linear susceptibility of a weak cavity field is obtained and $N-1$ transparency windows are observed. In the model we consider, no external fields are required to induce the transparency and the CIT effect is fully generated by cavity QED photons. We also compare the numerical integration of density-matrix equations with the analytical solutions provided by the quantum-jump approach and show that both results are in excellent agreement.

DOI: 10.1103/PhysRevA.109.023719

I. INTRODUCTION

Electromagnetically induced transparency (EIT) is a phenomenon that leads to absorption-free propagation of the probe field in the medium. This phenomenon is interpreted as a quantum destructive interference between two different excitation pathways to the upper level in three-level atomic systems [1,2]. As an extension of EIT, it has also been shown that the probe absorption spectrum in a four-level atomic system can exhibit two EIT windows, separated by a sharp absorption peak [3–5], and such a phenomenon is known as double EIT. It is demonstrated, both theoretically and experimentally, that the use of EIT can boost more control capabilities for the optical response of the material, resulting in numerous applications in nonlinear optics and quantum information processing [6–18].

Optical cavities provide an enhanced matter-light interaction and can be a more ideal and feasible platform to manipulate and control the matter-light interaction (see, e.g., Refs. [19–22]). Merging EIT with optical cavities (cavity EIT) consequently results in an effective increase in the enhancement of the main features of EIT [23,24]. Prediction and observation of EIT phenomena in a single atom inside an optical cavity can be traced back to Rice and Brecha [25], who termed this effect as cavity-induced transparency (CIT). They found that the absorption spectrum of the atom may exhibit a dip at the line center for a weak probe when the atom-cavity coupling strength is large compared to the cavity linewidth but smaller than the atom's free-space linewidth.

In this paper, we investigate the fully quantized description of Ref. [25] adopting the quantum-jump approach [26–28]. We also extend the CIT system to a four-level atomic system and observe two CIT windows (we refer to this effect as double CIT). In this method, it is the cavity field modes that couple the atomic transitions and no external fields whatsoever are required.

In this paper, we consider a four-level tripod-type structure for the atomic energy levels. This atomic structure has been extensively studied during the past decades. In particular, it has been extensively used to study the closely related phenomena, namely coherent population trapping (CPT) and electromagnetically induced transparency (EIT). As an application of CPT, it has been shown that four-level tripod-linked systems can have two degenerate adiabatic dark states, and thus these systems can be used to extend the ordinary three-level stimulated Raman adiabatic passage (STIRAP) technique for generating a quantum superposition of metastable states out of a single initial state [29]. Since dark states in these systems have no component of the excited intermediate state, they are immune to the atomic spontaneous decay. Under certain conditions these systems can be used for efficient nonlinear frequency generation when a medium is initially prepared in a coherent superposition [3]. It is also demonstrated that four-level tripod configurations can exhibit two EIT windows. Various EIT-related effects in these systems have been extensively studied, both theoretically and experimentally [3,4,17,30,31]. For applications in quantum information processing (QIP), a tripod system provides a means to entangle a pair of very weak optical fields in an atomic sample [32] and therefore can be used in schemes for QIP implementations. In Ref. [33], for example, an enhanced cross-Kerr nonlinearity occurring in a four-atomic-tripod configuration has been employed to realize a universal two-qubit quantum gate.

The structure of the paper is as follows. We introduce the system in Sec. II, describe the quantum-jump approach, give the time evolutions of the probability amplitudes in the system, and then derive the susceptibility of the atom-cavity systems. Note that we first investigate the double-CIT effect and then describe the single-CIT effect as a special case of the double-CIT effect. In Sec. III we study the CIT effects with susceptibilities of the weak cavity field in three- and four-level atomic systems, and then compare the numerical results of absorption with analytical solutions. Finally, we conclude the paper in Sec. IV with a summary.

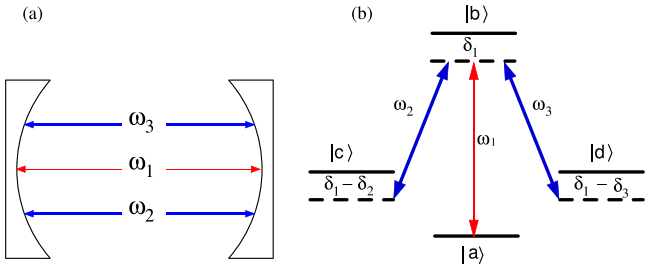

FIG. 1. Scheme of a double-cavity-induced transparency (double-CIT). (a) Three-mode optical cavity with resonant frequencies ω_1, ω_2, and ω_3. There is only one cavity photon in mode of frequency ω_1 to raise the atomic state from $|a\rangle$. (b) Tripod-type four-level configuration with levels $|a\rangle$, $|c\rangle$, and $|d\rangle$ are lower-energy states, each coupled to a common high-energy state $|b\rangle$. The field of frequency ω_1 interacting with the atom on the $|a\rangle \leftrightarrow |b\rangle$ transition is weak compared to the fields of frequencies ω_2 and ω_3 acting on the transitions $|c\rangle \leftrightarrow |b\rangle$ and $|d\rangle \leftrightarrow |b\rangle$, respectively.

II. THEORETICAL BACKGROUND

A. The four-level tripod-type atomic system

In Fig. 1, we consider a four-level tripod-type atom consisting of the atomic levels $|a\rangle$, $|c\rangle$, and $|d\rangle$ each coupled simultaneously to a common excited state $|b\rangle$ via a dipole-allowed transition but not to each other. The atom interacts with three electromagnetic (EM) modes inside a high Q cavity with only one photon in its mode. These three modes have the resonant frequencies ω_1, ω_2, and ω_3 and the atomic levels are such that $\omega_{ba} = \omega_1 + \delta_1$, $\omega_{bc} = \omega_2 + \delta_2$, and $\omega_{bd} = \omega_3 + \delta_3$. For an atom with such a configuration in the state $|a\rangle$ interacting with potentially three cavity modes and one photon, the initial state is chosen to be $|a, 1_1, 0_2, 0_3\rangle$, where there is only one cavity photon available in the first mode to raise the atomic state from $|a\rangle$. Here, we use the notation $|\alpha\rangle \otimes |\beta_1\rangle \otimes |\beta_2\rangle \otimes |\beta_3\rangle \equiv |\alpha, \beta_1, \beta_2, \beta_3\rangle$ where $|\alpha\rangle$ ($\alpha = a, b, c, d$) represents the atomic state, while $|\beta_i\rangle$ (for $i = 1, 2, 3$) denotes that the cavity fields have a β photon in mode i with ($\beta \in 0, 1$).

Under the dipole and rotating-wave approximations and in the Schrödinger picture, the Hamiltonian describing the system in Fig. 1 is

$$H = \hbar \sum_{i=a,b,c,d} \omega_i \hat{\sigma}_{ii} + \hbar \sum_{j=1}^{3} \omega_j \hat{a}_j^\dagger \hat{a}_j + \hbar[g_1 \hat{a}_1 \hat{\sigma}_{ba} + g_2 \hat{\sigma}_{cb} \hat{a}_2^\dagger + g_3 \hat{a}_3 \hat{\sigma}_{bd} + \text{H.c.}], \quad (1)$$

where the coupling constants are g_j ($j = 1, 2, 3$), the atomic operators $\hat{\sigma}_{ba} \equiv |b\rangle\langle a|$, $\hat{\sigma}_{cb} \equiv |c\rangle\langle b|$, and $\hat{\sigma}_{bd} \equiv |b\rangle\langle d|$, and $\hat{a}_j$ is the photon annihilation operator for the cavity mode. In the interaction picture, the tripod Hamiltonian H_{int} is expressed, with $|a, 1_1, 0_2, 0_3\rangle$ to be the zero-point energy and in matrix form, by ($\hbar = 1$)

$$H_{\text{int}} = \begin{bmatrix} 0 & g_1 & 0 & 0 \\ g_1 & \delta_1 & g_2 & g_3 \\ 0 & g_2 & \delta_1 - \delta_2 & 0 \\ 0 & g_3 & 0 & \delta_1 - \delta_3 \end{bmatrix}, \quad (2)$$

in the four-state basis $\{|a, 1_1, 0_2, 0_3\rangle, |b, 0_1, 0_2, 0_3\rangle, |c, 0_1, 1_2, 0_3\rangle, |d, 0_1, 0_2, 1_3\rangle\}$.

As discussed in later sections and for the purpose of this paper, we set the field of frequency ω_1 interacting with the atom on the $|a\rangle \leftrightarrow |b\rangle$ transition to be weak compared to the fields of frequencies ω_2 and ω_3 acting on the transitions $|c\rangle \leftrightarrow |b\rangle$ and $|d\rangle \leftrightarrow |b\rangle$, respectively (see Fig. 1).

B. Density-matrix equation of motion

Our main goal in this paper is to investigate theoretically the generation of a double-CIT effect in cavity QED. To this end, one can follow the standard density-matrix method, including atomic and photonic decays, to derive the optical Bloch equations for the four-level tripod system in Fig. 1. Considering this approach and taking into account the dissipative mechanisms in the system (2), the time evolution is given, in the density-matrix framework, as

$$\frac{\partial}{\partial t}\rho = -i[H_{\text{int}}, \rho] + \mathcal{L}\rho. \quad (3)$$

The first term in Eq. (3) describes the atom-field coupling for the system H_{int} in Eq. (2) and the second term $\mathcal{L}\rho$ is known as Liouville's operator and contains the effects of dissipations. At zero temperature, the Liouvillian $\mathcal{L}\rho$ has the so-called Lindblad form

$$\mathcal{L}\rho = \sum_i \eta_i \mathcal{D}_i \rho \mathcal{D}_i^\dagger - \frac{1}{2} \sum_i \eta_i (\mathcal{D}_i^\dagger \mathcal{D}_i \rho + \rho \mathcal{D}_i^\dagger \mathcal{D}_i), \quad (4)$$

where η represents the loss of population. In our case η may refer to the spontaneous emission γ or to the cavity field rate κ. The operators $\mathcal{D}$ and $\mathcal{D}^\dagger$ are the corresponding system operators. To study the susceptibility χ of the atom, one finds the steady-state solutions when certain conditions of adiabaticity and moderate intensities of the cavity fields are valid (such conditions will be determined later). The susceptibility is related to the coherency ρ_{ba} and the weak cavity field E_1 by the relation [34]

$$\chi = (N|\mu_{ba}|/\epsilon_0 E_1)\rho_{ab}, \quad (5)$$

with N is the number of density of atoms and μ_{ba} is the dipole moment of the underlying weak (probelike) transition. However, this procedure is quite cumbersome and impractical, and we will use this procedure for numerical solutions. Instead, we will discuss in the following section a much simpler way to describe the system via the quantum-jump method.

C. Quantum-jump approach

Applying the general master equation in Eq. (3) on our system shows that the system is not closed and both the atomic and photonic decays in the system result in an irreversible loss of population. For example, the decay of the cavity field from the state $|a, 1_1, 0_2, 0_3\rangle$ takes the system to state $|a, 0_1, 0_2, 0_3\rangle$ and the decay of state $|b, 0_1, 0_2, 0_3\rangle$ due to the atomic relaxation can take the system to one of the states $|c, 0_1, 0_2, 0_3\rangle$ or $|d, 0_1, 0_2, 0_3\rangle$. As the Hamiltonian in Eq. (2) acts in the Hilbert space $\mathbb{H} = \{|a, 1_1, 0_2, 0_3\rangle, |b, 0_1, 0_2, 0_3\rangle, |c, 0_1, 1_2, 0_3\rangle, |d, 0_1, 0_2, 1_3\rangle\}$, the states $|a, 0_1, 0_2, 0_3\rangle$, $|c, 0_1, 0_2, 0_3\rangle$, and $|d, 0_1, 0_2, 0_3\rangle$ are not in space $\mathbb{H}$, which means we have a system that is not closed and both decay channels result in an irreversible loss of population. This being the case, we can apply the

quantum-jump approach as a description of the system instead of the master-equation method. This approach has been used in earlier work for applications in quantum information processing [35–37].

For convenience, we rewrite the previous Liouville's equation as (see Appendix A)

$$\frac{\partial}{\partial t}\rho = -i(H'\rho - \rho H'^{\dagger}) + J\rho, \tag{6}$$

where $H' = H_{\rm int} - \frac{i}{2}\sum_i \eta_i \mathcal{D}_i^{\dagger}\mathcal{D}_i$ and $J\rho = \sum_i \eta_i \mathcal{D}_i \rho \mathcal{D}_i^{\dagger}$. Equation (6) shows that the time evolution of the density operator in Eq. (3) has two contributions. The first one is due to the effective Hamiltonian H', while the second one is due to the so-called jump superoperator $J\rho$. As decays in our system result in an irreversible loss of population, we can propagate the wave function $|\psi(t)\rangle$ (instead of the density matrix ρ) with the Schrödinger equation using the non-Hermitian Hamiltonian H', i.e., $i\frac{\partial}{\partial t}|\psi(t)\rangle = H'|\psi(t)\rangle$. The Hamiltonian H' describing the system when decays to be considered is

$$H' = \begin{bmatrix} -i\frac{\kappa_1}{2} & g_1 & 0 & 0 \\ g_1 & \delta_1 - i\frac{\gamma_{ba}}{2} & g_2 & g_3 \\ 0 & g_2 & (\delta_1-\delta_2) - i\frac{\kappa_2}{2} & 0 \\ 0 & g_3 & 0 & (\delta_1-\delta_3) - i\frac{\kappa_3}{2} \end{bmatrix}, \tag{7}$$

where κ_1, κ_2, and κ_3 are the decays of the cavity fields and γ_{ba} is the atomic relaxation from state $|b\rangle$ to state $|a\rangle$. Under the CIT conditions (which are discussed later in the following sections), atom relaxations from state $|b\rangle$ to state $|c\rangle$ and from state $|b\rangle$ to state $|d\rangle$ have been neglected as they are sufficiently small compared to γ_{ba}. The time evolution of the probability amplitudes in the system $|\psi(t)\rangle = C_a|a,1_1,0_2,0_3\rangle + C_b|b,0_1,0_2,0_3\rangle + C_c|c,0_1,1_2,0_3\rangle + C_d|d,0_1,0_2,1_3\rangle$ (where we choose $|a,1_1,0_2,0_3\rangle$ as an initial state) is given by

$$i\dot{C}_a = -i\frac{\kappa_1}{2}C_a + g_1 C_b, \tag{8a}$$

$$i\dot{C}_b = \left[\delta_1 - i\frac{\gamma_{ba}}{2}\right]C_b + g_1 C_a + g_2 C_c + g_3 C_d, \tag{8b}$$

$$i\dot{C}_c = \left[(\delta_1-\delta_2) - i\frac{\kappa_2}{2}\right]C_c + g_2 C_b, \tag{8c}$$

$$i\dot{C}_d = \left[(\delta_1-\delta_3) - i\frac{\kappa_3}{2}\right]C_d + g_3 C_b. \tag{8d}$$

In calculating the optical susceptibility of the tripod atom in Fig. 1, the quantity of interest is the off-diagonal steady-state density-matrix element ρ_{ab}. From the set of coupled differential Eqs. (8), equations of motion for the density-matrix elements are easily derived from $\dot{\rho}_{ij} = c_i\dot{c}_j^* + \dot{c}_i c_j^*$. One, therefore, can obtain the following set of linear equations (details can be found in Appendix B),

$$i\dot{\rho}_{ab} = -\left[\delta_1 + \frac{i}{2}(\gamma_{ba}+\kappa_1)\right]\rho_{ab} + g_1(\rho_{bb}-\rho_{aa}) - g_2\rho_{ac} - g_3\rho_{ad}, \tag{9a}$$

$$i\dot{\rho}_{ac} = -\left[(\delta_1-\delta_2) + \frac{i}{2}(\kappa_1+\kappa_2)\right]\rho_{ac} + g_1\rho_{bc} - g_2\rho_{ab}, \tag{9b}$$

$$i\dot{\rho}_{ad} = -\left[(\delta_1-\delta_3) + \frac{i}{2}(\kappa_1+\kappa_3)\right]\rho_{ad} + g_1\rho_{bd} - g_3\rho_{ab}. \tag{9c}$$

In the stationary regime $[\dot{\rho}(t)_{ij} = 0]$, from Eqs. (9b) and (9c) we have $\rho_{ac} = \{-g_2/[(\delta_1-\delta_2) + \frac{i}{2}(\kappa_1+\kappa_2)]\}\rho_{ab}$ and $\rho_{ad} = \{-g_3/[(\delta_1-\delta_3) + \frac{i}{2}(\kappa_1+\kappa_3)]\}\rho_{ab}$, where the terms containing $g_1\rho_{bc}$ and $g_1\rho_{bd}$ have been neglected due to the smallness of g_1, ρ_{bc}, and ρ_{bd}. Substituting ρ_{ac} and ρ_{ad} into (9a) and taking $\rho_{bb} - \rho_{aa} \simeq -1$ as the field of frequency ω_1 is assumed too weak [7], we obtain

$$\rho_{ab} = -\frac{g_1}{\left[\delta_1 + \frac{i}{2}(\gamma_{ba}+\kappa_1)\right] - g_2^2\left[(\delta_1-\delta_2) + \frac{i}{2}(\kappa_1+\kappa_2)\right]^{-1} - g_3^2\left[(\delta_1-\delta_3) + \frac{i}{2}(\kappa_1+\kappa_3)\right]^{-1}}. \tag{10}$$

As the specific details of the physical system are not of our concern here, we replace the susceptibility χ in Eq. (5) with a reduced susceptibility. Then, for CIT it reads $\tilde{\chi} = \rho_{ab}$. Thus, it is the imaginary part of ρ_{ab} that gives the main characteristics of the absorption spectrum and therefore the essential features of CIT.

III. CAVITY-INDUCED TRANSPARENCY

We now introduce the main characteristics of CIT by means of the absorption spectrum. Considering the reduced susceptibility of the atom-cavity system described in the previous section, the imaginary part of $\tilde{\chi}$ is depicted in Fig. 2. We first consider a case of vanishing coupling $g_3/\gamma_{ba} = 0$, reducing thus the four-level tripod-configuration system in Fig. 1 to a three-level Λ-type atom coupled to two cavity modes. In this case, the atomic transition $|a\rangle \leftrightarrow |b\rangle$ is weakly coupled by the cavity mode of frequency ω_1 and the atomic transition $|b\rangle \leftrightarrow |c\rangle$ is strongly coupled by the cavity field of frequency ω_2. For perfect resonance $\omega_2 = \omega_{bc}$ and under the condition $\gamma_{ba} > g_2 \gg \kappa_{1,2}$, a single-cavity-induced transparency (single-CIT) is observed, as illustrated in Fig. 2(a). This effect was first studied by Rice and Brecha [25], and they showed that a system consisting of a single two-level atom inside an optical cavity can exhibit a dip in absorption at the line center. In their single-CIT model, a weak classical field is required to be coupled directly to the atom. In the system we consider, however, we show that the single-CIT effect can also be generated by a three-level Λ-type atom interacting with two modes inside a cavity. In this model, it is g_1 that plays the role of the weak-coupling field; hence no classical field is required. Similarly, it is important to satisfy the condition $\gamma_{ba} > g_2 \gg \kappa_{1,2}$ for the single-CIT effect to occur. In Fig. 2(a), with $\delta_2 = 0$ the absorption spectrum is plotted for the cases of $g_2 = 0.5\gamma_{ba}$ (black) and $g_2 = 0.75\gamma_{ba}$ (gray). As seen, the spectrum is split into two peaks separated

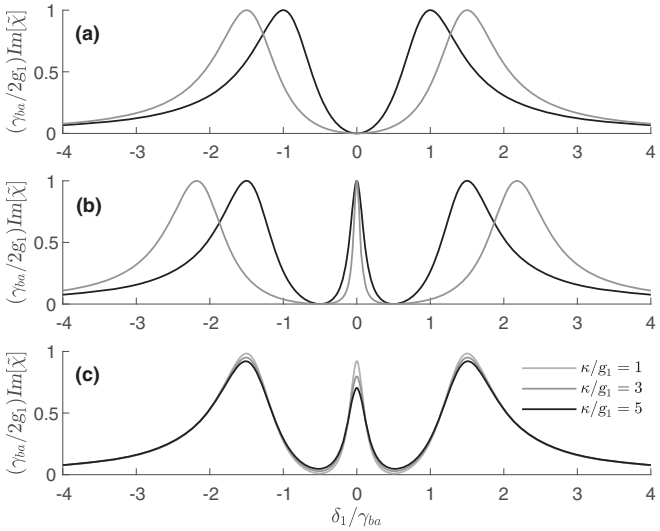

FIG. 2. Plots of absorption spectrum as a function of normalized weak (probelike) detuning. Cavity decays κ_1, κ_2, and κ_3 are all set to κ and $\kappa/\gamma_{ba} = 10^{-5}$. (a) Single-CIT effect with $g_2/\gamma_{ba} = 0.5$ (black) and $g_2/\gamma_{ba} = 0.75$ (gray). Only two cavity modes ω_1 and ω_2 are considered in the atom-cavity system (see Fig. 1), and the cavity field ω_2 is tuned to the atomic transition $|b\rangle \leftrightarrow |c\rangle$, $\omega_2 = \omega_{bc}$. (b) Double-CIT effect with the couplings g_2 and g_3 are set to g and $g/\gamma_{ba} = 0.5$ (black) and $g/\gamma_{ba} = 0.75$ (gray). The detunings δ_2 and δ_3 are set to δ and $\delta/\gamma_{ba} = 0.25$. (c) Damped double-CIT peaks for the case of $g/\gamma_{ba} = 0.5$. The cavity decays are in the limit of $g_1 \leqslant \kappa \ll g_{2,3}$. In all plots $g_1 \ll g_{2,3}$ and $\gamma_{ba} > g_{2,3} \gg \kappa$.

by $2g_2$, which is known as the Autler-Towns splitting. At the line center, the atom becomes transparent to the resonant field.

The case of double-cavity-induced transparency (double-CIT) is shown in Fig. 2(b). In this case, we set the detunings δ_2 and δ_3 to δ with $\delta_2 = -\delta_3$ and the coupling constants g_2 and g_3 are all set to g. Under the condition $\gamma_{ba} > g \gg \kappa_{1,2,3}$ we plot the absorption profile as a function of the normalized weak (probelike) detuning, and a double-CIT effect is observed. As seen in Fig. 2(b), the absorption spectrum has minima at $\delta_1 = \pm\delta$ (CIT windows) and maxima at the line center ($\delta_1 = 0$) and at Autler-Towns peaks ($\delta_1 = \pm\sqrt{2g^2 + \delta^2}$). Setting $\delta/\gamma_{ba} = 0.25$ and increasing the coupling g from $g = 0.5\gamma_{ba}$ (black) to $g = 0.75\gamma_{ba}$ (gray) result in a larger splitting between the left and right side peaks with the same linewidths, a narrow central peak, and a broader two CIT dips. The two transparency dips display that the weak (probelike) cavity field could be simultaneously transparent at two symmetric frequencies, while the absorption peak at the line center implies that the weak field is fully absorbed by the system. In all cases presented above, the cavity decays κ_1, κ_2, and κ_3 are all set to κ and the condition $g_{1,2,3} \gg \kappa$ is satisfied. In the limit $g_1 \leqslant \kappa \ll g_{2,3}$, it is immediately clear that the losses have a dramatic effect on the central peak (at $\delta_1 = 0$) and its amplitude is heavily suppressed for even small values of κ. The Autler-Towns peaks, by contrast, are modified only slightly [see Fig. 2(c)]. We can understand this by considering the double-CIT conditions (where $\gamma_{ba} > g \gg \kappa_{1,2,3}$ and $g_{2,3} \gg g_1$) and the decay channels in the tripod-configuration model schematically shown in Fig. 1. The double-CIT

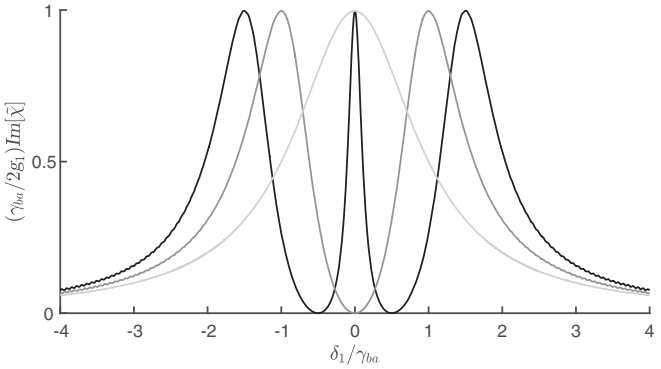

FIG. 3. Numerical results for absorption spectrum as a function of normalized detuning δ_1/γ_{ba} for $\gamma_{bc}/\gamma_{ba} = \gamma_{bd}/\gamma_{ba} = 10^{-3}$. The light-gray curve corresponds to the case of $g_{2,3} = 0$ (two-level atom). For the case of $g/\gamma_{ba} = 0.5$, the gray and black curves represent the numerical results for the single- and double-CIT, respectively, with the same parameters as in Figs. 2(a) and 2(b) (black curves).

features presented here mimic the double-EIT features presented by the tripod systems driven by a weak and tunable probe field in the presence of two strong pump lasers. In this model, however, no external fields whatsoever are required to induce the transparency and double-CIT effect is fully generated by cavity QED photons.

In analogy with systems exhibiting the double-EIT effect, the double-CIT effect is a quantum interference process leading to the cancellation of the absorption of a weak cavity field by applying strong cavity fields in the same medium. This quantum interference effect arises from different transition pathways of cavity fields to the upper level. As a result of the destructive interference between these different transition pathways, the atom inside the cavity exhibits three absorption peaks. Alternatively this can be viewed by the dressed-state picture. In this picture the strong fields create dressed states, and the contributions from these dressed states are equal but with opposite signs, leading to two dips in the absorption spectrum.

We have tested previous theoretical results by numerically integrating the full set of Bloch equations for the atomic density-matrix elements taking into account all possible decay channels predicted by the Liouville equation in the compound system. It is illustrated in Fig. 3 that the absorption spectrum by the analytical formula in Eq. (10) is practically indistinguishable from the exact numerical calculations.

IV. CONCLUSION

In summary, a fully quantized atom-cavity model is proposed for generating single- and double-cavity-induced transparency by cavity QED photons. To bypass the analytical solution of the equations of motion of the atomic density-matrix elements, we introduce the quantum-jump approach. As the master-equation method shows that there is a large number of quantum levels involved, we have seen that the quantum-jump approach greatly simplifies the calculations by dealing with the system wave function and looking for the evolution of the four variables in Eqs. (8). Comparing the numerical integration of the density-matrix equations with

the analytical solutions provided by the quantum-jump method, we have shown that both methods are in excellent agreement.

For generating the double-CIT effect, we show that this effect can be produced by a system of tripod-type four-level atoms interacting with three cavity modes. Only one of these cavity modes has an excitation so that it raises the system from $|a\rangle$ to $|b\rangle$, and is chosen to be the weak (probelike) field. As the two remaining empty modes couple to the same upper level $|b\rangle$, they can have similar frequencies if the lower levels $|c\rangle$ and $|d\rangle$ are closely spaced in energy, which is the case for most of the alkali atoms. We thus assume (for simplicity) equal values for couplings g_2 and g_3 and detunings δ_2 and δ_3 in Figs. 2 and 3. We also show that the single-CIT effect can be realized. To form this effect we actually cancel one transition from the double-CIT system (we choose to cancel the atomic transition $|b\rangle \leftrightarrow |d\rangle$), so that a Λ-type three-level atom interacts with a bimodal cavity. In this case, we use the double-CIT weak field containing an excitation to excite the atom from the state $|a\rangle$ to the state $|b\rangle$, and select the empty mode ω_2 to couple the atomic transition $|b\rangle \rightarrow |c\rangle$. In all cases, the CIT condition $\gamma_{ba} > g \gg \kappa$ and the weak limit $g_1 \ll g$ must be satisfied.

Finally, in this work we consider a simultaneous interaction between a multimode field and a multilevel atom inside one cavity. This kind of cavity-atom interaction can be achievable with recent rapid and remarkable developments in the resonator systems. For example, advanced developments in micro- and nanofabrication technologies allow direct and precise integration of nanostructures into whispering-gallery-mode (WGMs) microcavities, resulting in strong coupling between different types of modes, also named supermodes, in WGM microcavities, and plasmonic nanostructures [38]. In fact, with remarkable progress in the fabrication strategies of optical microcavities and plasmonic nanostructures [23,38], it is promising that the multiphoton cavity resonances can be in the range of practicality.

ACKNOWLEDGMENTS

The author would like to thank Dr. M. Tohari for helpful discussions and comments on the manuscript. This work is supported by Scientific Research Deanship (SRD) at King Khalid University (KKU), Saudi Arabia.

APPENDIX A: THE NON-HERMITIAN EFFECTIVE HAMILTONIAN

In general, the time evolution of the system (2) is governed by the master equation

$$\frac{\partial}{\partial t}\rho = -i[H_{\rm int}, \rho] + \mathcal{L}\rho, \tag{A1}$$

where $H_{\rm int}$ is the Hermitian Hamiltonian of the system, while $\mathcal{L}\rho$ is the Liouville's operator containing the effects of dissipations. At zero temperature, the Liouvillian $\mathcal{L}\rho$ has the so-called Lindblad form

$$\mathcal{L}\rho = \sum_i \eta_i \mathcal{D}_i \rho \mathcal{D}_i^\dagger - \frac{1}{2}\sum_i \eta_i (\mathcal{D}_i^\dagger \mathcal{D}_i \rho + \rho \mathcal{D}_i^\dagger \mathcal{D}_i), \tag{A2}$$

where η represents the loss of population. In our case η may refer to the spontaneous emission γ or to the cavity field rate κ. The operators $\mathcal{D}$ and $\mathcal{D}^\dagger$ are the corresponding system operators.

As the system we consider here is not closed and all decay channels in the system result in an irreversible loss of population (see Sec. II C), we can apply the wave-function approach in Refs. [26,27] to study the evolution of the system instead of the standard master-equation approach. Following the procedure in the wave-function approach, we define a non-Hermitian effective Hamiltonian of the system through

$$H' = H_{\rm int} - \frac{i}{2}\sum_i \eta_i \mathcal{D}_i^\dagger \mathcal{D}_i, \tag{A3}$$

and the so-called jump superoperator

$$\mathcal{L}_{\rm jump}\rho = \sum_i \eta_i \mathcal{D}_i \rho \mathcal{D}_i^\dagger, \tag{A4}$$

in terms of which the master equation (A1) can be cast in the form

$$\frac{\partial}{\partial t}\rho = -i\,(H'\rho - \rho H'^\dagger) + \mathcal{L}_{\rm jump}\rho. \tag{A5}$$

According to the wave-function approach, we can propagate the state vector of the system $|\psi(t)\rangle = C_a|a, 1_1, 0_2, 0_3\rangle + C_b|b, 0_1, 0_2, 0_3\rangle + C_c|c, 0_1, 1_2, 0_3\rangle + C_d|d, 0_1, 0_2, 1_3\rangle$ with the Schrödinger equation using the non-Hermitian effective Hamiltonian (A3), which yields the differential Eqs. (8). Here, we replace the usual master equation for the system by a wave-function evolution. This treatment clearly simplifies the calculations on the problem which would otherwise be exceedingly complicated.

APPENDIX B: THE EXPRESSION OF THE STEADY-STATE LINEAR SUSCEPTIBILITY

Applying the wave-function approach, we substitute the non-Hermitian effective Hamiltonian (A3) and state vector $|\psi(t)\rangle$ into the time-dependent Schrödinger equation and obtain the amplitude equations

$$i\dot{C}_a = -i\frac{\kappa_1}{2}C_a + g_1 C_b, \tag{B1a}$$

$$i\dot{C}_b = \left[\delta_1 - i\frac{\gamma_{ba}}{2}\right]C_b + g_1 C_a + g_2 C_c + g_3 C_d, \tag{B1b}$$

$$i\dot{C}_c = \left[(\delta_1 - \delta_2) - i\frac{\kappa_2}{2}\right]C_c + g_2 C_b, \tag{B1c}$$

$$i\dot{C}_d = \left[(\delta_1 - \delta_3) - i\frac{\kappa_3}{2}\right]C_d + g_3 C_b. \tag{B1d}$$

In the steady-state limit the reduced susceptibility is $\tilde{\chi} = \rho_{ab}$, where $\rho_{ab} \equiv C_a(\infty)C_b^*(\infty)$. We can find an expression for ρ_{ab} by using the amplitude equations (B1) to derive the equations of motion for the density-matrix elements from

$$\dot{\rho}_{ij} = C_i(\dot{C}_j^*) + (\dot{C}_i)C_j^*. \tag{B2}$$

From this equation $\dot{\rho}_{ab} = C_a(\dot{C}_b^*) + (\dot{C}_a)C_b^*$. Thus, with substitution from Eqs. (B1a) and (B1b), it follows that

$$i\dot{\rho}_{ab} = -\left[\delta_1 + \frac{i}{2}(\gamma_{ba} + \kappa_1)\right]\rho_{ab} + g_1(\rho_{bb} - \rho_{aa}) - g_2\rho_{ac} - g_3\rho_{ad}. \tag{B3}$$

Similarly, we use Eqs. (B1a) and (B1c) for obtaining $\dot{\rho}_{ac}$ and Eqs. (B1a) and (B1d) for finding $\dot{\rho}_{ad}$. One then finds that

$$i\dot{\rho}_{ac} = -\left[(\delta_1 - \delta_2) + \frac{i}{2}(\kappa_1 + \kappa_2)\right]\rho_{ac} + g_1\rho_{bc} - g_2\rho_{ab}, \tag{B4a}$$

$$i\dot{\rho}_{ad} = -\left[(\delta_1 - \delta_3) + \frac{i}{2}(\kappa_1 + \kappa_3)\right]\rho_{ad} + g_1\rho_{bd} - g_3\rho_{ab}. \tag{B4b}$$

Due to the smallness of g_1, ρ_{bc}, and ρ_{bd}, the terms containing $g_1\rho_{bc}$ and $g_1\rho_{bd}$ in Eqs. (B4a) and (B4b) can be neglected. In the stationary regime ($\dot{\rho}(t)_{ij} = 0$), we have

$$\rho_{ac} = \left\{-g_2 \Big/ \left[(\delta_1 - \delta_2) + \frac{i}{2}(\kappa_1 + \kappa_2)\right]\right\}\rho_{ab}, \tag{B5a}$$

$$\rho_{ad} = \left\{-g_3 \Big/ \left[(\delta_1 - \delta_3) + \frac{i}{2}(\kappa_1 + \kappa_3)\right]\right\}\rho_{ab}. \tag{B5b}$$

Substituting ρ_{ac} and ρ_{bd} into (B3), dropping the time derivative, and taking $\rho_{bb} - \rho_{aa} \simeq -1$ as the field of frequency ω_1 is assumed too weak, one can easily obtain ρ_{ab} in Eq. (10).

[1] J. E. Field, K. H. Hahn, and S. E. Harris, Observation of electromagnetically induced transparency in collisionally broadened lead vapor, Phys. Rev. Lett. **67**, 3062 (1991).

[2] S. E. Harris, Electromagnetically induced transparency, Phys. Today **50** (7), 36 (1997).

[3] E. Paspalakis and P. L. Knight, Transparency, slow light and enhanced nonlinear optics in a four-level scheme, J. Opt. B: Quantum Semiclass. Opt. **4**, S372 (2002).

[4] E. Paspalakis and P. L. Knight, Transparency and parametric generation in a four-level system, J. Mod. Opt. **49**, 87 (2002).

[5] L. Safari, D. Iablonskyi, and F. Fratini, Double-electromagnetically induced transparency in a Y-type atomic system, Eur. Phys. J. D **68**, 27 (2014).

[6] R. G. Beausoleil, W. J. Munro, D. A. Rodrigues, and T. P. Spiller, Applications of electromagnetically induced transparency to quantum information processing, J. Mod. Opt. **51**, 2441 (2004).

[7] M. Fleischhauer, A. Imamoglu, and J. P. Marangos, Electromagnetically induced transparency: Optics in coherent media, Rev. Mod. Phys. **77**, 633 (2005).

[8] U. Schnorrberger, J. D. Thompson, S. Trotzky, R. Pugatch, N. Davidson, S. Kuhr, and I. Bloch, Electromagnetically induced transparency and light storage in an atomic Mott insulator, Phys. Rev. Lett. **103**, 033003 (2009).

[9] X. Yang, M. Yu, D.-L. Kwong, and C. W. Wong, All-optical analog to electromagnetically induced transparency in multiple coupled photonic crystal cavities, Phys. Rev. Lett. **102**, 173902 (2009).

[10] X. Liu, R. Gu, J. Singh, Y. Ma, Z. Zhu, J. Tian, M. He, J. Han, and W. Zhang, Electromagnetically induced transparency in terahertz plasmonic metamaterials via dual excitation pathways of the dark mode, Appl. Phys. Lett. **100**, 131101 (2012).

[11] M. Himsworth, P. Nisbet, J. Dilley, G. Langfahl-Klabes, and A. Kuhn, EIT-based quantum memory for single photons from cavity-QED, Appl. Phys. B **103**, 579 (2011).

[12] I. Novikova, R. L. Walsworth, and Y. Xiao, Electromagnetically induced transparency-based slow and stored light in warm atoms, Laser Photon. Rev. **6**, 333 (2012).

[13] Y. Yang, I. I. Kravchenko, D. P. Briggs, and J. Valentine, All-dielectric metasurface analogue of electromagnetically induced transparency, Nat. Commun. **5**, 5753 (2014).

[14] H. S. Borges and C. J. Villas-Bôas, Quantum phase gate based on electromagnetically induced transparency in optical cavities, Phys. Rev. A **94**, 052337 (2016).

[15] Y.-C. Liu, B.-B. Li, and Y.-F. Xiao, Electromagnetically induced transparency in optical microcavities, Nanophotonics **6**, 789 (2017).

[16] M. Paternostro, M. S. Kim, and B. S. Ham, Generation of entangled coherent states via cross-phase-modulation in a double electromagnetically induced transparency regime, Phys. Rev. A **67**, 023811 (2003).

[17] S. Li, X. Yang, X. Cao, C. Zhang, C. Xie, and H. Wang, Enhanced cross-phase modulation based on a double electromagnetically induced transparency in a four-level tripod atomic system, Phys. Rev. Lett. **101**, 073602 (2008).

[18] H. M. M. Alotaibi and B. C. Sanders, Double-double electromagnetically induced transparency with amplification, Phys. Rev. A **89**, 021802(R) (2014).

[19] H. Mabuchi and A. C. Doherty, Cavity quantum electrodynamics: Coherence in context, Science **298**, 1372 (2002).

[20] S. Haroche and J.-M. Raimond, *Exploring the Quantum: Atoms, Cavities, and Photons* (Oxford University Press, Oxford, UK, 2013).

[21] P. F. Herskind, A. Dantan, J. P. Marler, M. Albert, and M. Drewsen, Realization of collective strong coupling with ion Coulomb crystals in an optical cavity, Nat. Phys. **5**, 494 (2009).

[22] I. Favero and K. Karrai, Optomechanics of deformable optical cavities, Nat. Photon. **3**, 201 (2009).

[23] For a review of EIT in optical cavities, see H. Qin, M. Ding, and Y. Yin, Induced transparency with optical cavities, Adv. Photon. Res. **1**, 2000009 (2020).

[24] M. Mücke, E. Figueroa, J. Bochmann, C. Hahn, K. Murr, S. Ritter, C. J. Villas-Boas, and G. Rempe, Electromagnetically induced transparency with single atoms in a cavity, Nature (London) **465**, 755 (2010).

[25] P. R. Rice and R. J. Brecha, Cavity induced transparency, Opt. Commun. **126**, 230 (1996).

[26] J. Dalibard, Y. Castin, and K. Mølmer, Wave-function approach to dissipative processes in quantum optics, Phys. Rev. Lett. **68**, 580 (1992).

[27] K. Mølmer, Y. Castin, and J. Dalibard, Monte Carlo wave-function method in quantum optics, J. Opt. Soc. Am. B **10**, 524 (1993).

[28] C. C. Gerry and P. L. Knight, *Introductory Quantum Optics* (Cambridge University Press, Cambridge, UK, 2005).

[29] R. Unanyan, M. Fleischhauer, B. W. Shore, and K. Bergmann, Robust creation and phase-sensitive probing of superposition

states via stimulated Raman adiabatic passage (STIRAP) with degenerate dark states, Opt. Commun. **155**, 144 (1998).

[30] B. S. Ham and P. R. Hemmer, Coherence switching in a four-level system: Quantum switching, Phys. Rev. Lett. **84**, 4080 (2000).

[31] A. Raczyński, M. Rzepecka, J. Zaremba, and S. Zielińska-Kaniasty, Polariton picture of light propagation and storing in a tripod system, Opt. Commun. **260**, 73 (2006).

[32] D. Petrosyan and Y. P. Malakyan, Magneto-optical rotation and cross-phase modulation via coherently driven four-level atoms in a tripod configuration, Phys. Rev. A **70**, 023822 (2004).

[33] S. Rebić, D. Vitali, C. Ottaviani, P. Tombesi, M. Artoni, F. Cataliotti, and R. Corbalán, Polarization phase gate with a tripod atomic system, Phys. Rev. A **70**, 032317 (2004).

[34] M. Scully and M. Zubairy, *Quantum Optics* (Cambridge University Press, Cambridge, UK, 1997).

[35] M. M. Alqahtani, Multiphoton process in cavity QED photons for implementing a three-qubit quantum gate operation, Quantum Inf. Process. **19**, 12 (2020).

[36] M. M. Alqahtani, Quantum phase gate based on multiphoton process in multimode cavity QED, Quantum Inf. Process. **17**, 211(2018).

[37] M. M. Alqahtani, M. S. Everitt, and B. M Garraway, Cavity QED photons for quantum information processing, J. Phys. B: At. Mol. Opt. Phys. **55**, 184004 (2022).

[38] Y. Chen, Y. Yin, L. Ma, and O. G. Schmidt, Recent progress on optoplasmonic whispering-gallery-mode microcavities, Adv. Opt. Mater. **9**, 2100143 (2021).